

Multiphoton absorption and nonlinear refraction of GaAs in the mid-infrared

W. C. Hurlbut and Yun-Shik Lee

Department of Physics, Oregon State University, Corvallis, Oregon 97331-6507, USA

K. L. Vodopyanov, P. S. Kuo, and M. M. Fejer

E. L. Ginzton Laboratory, Stanford University, Stanford, California 94305, USA

Received August 28, 2006; revised December 5, 2006; accepted December 28, 2006;
posted January 4, 2007 (Doc. ID 74528); published February 15, 2007

We report the wavelength dependencies of the two- and three-photon absorption coefficients of undoped GaAs in the spectral range 1.3–3.5 μm , as well as nonlinear refractive index n_2 in the range 1.7–3.25 μm . The data were obtained by using the single-beam Z-scan method with 100-fs-long optical pulses. Anisotropy of the three-photon absorption coefficient was observed and found to be consistent with the crystal symmetry of GaAs. © 2007 Optical Society of America
OCIS codes: 190.4180, 190.3270, 320.4400.

Near-infrared nonlinear optical properties of gallium arsenide (GaAs), related to third-order susceptibility $\chi^{(3)}$, namely, two-photon absorption (2PA) and nonlinear refraction, have been widely studied in the past because of their importance for a variety of photonic devices, including ultrafast all-optical switches and optical power limiters.¹ However, in the mid-infrared, its optical properties related to $\chi^{(3)}$ and higher-order nonlinearities are not well characterized. The necessity of this study is dictated by the fact that new nonlinear optical applications of GaAs have emerged recently. In particular, orientation-patterned GaAs structures² show big promise for use in quasi-phase-matched frequency downconversion. A few examples of such applications include a broadly tunable mid-IR optical parametric oscillator,³ a supercontinuum generator,⁴ and a THz-wave source based on optical rectification of femtosecond pulses in orientation-patterned GaAs.^{5,6} 2PA, three-photon absorption (3PA), and the optical Kerr effect (related to the nonlinear refractive index, n_2) can severely limit performance of these devices at the high optical intensities required for their operation because of losses due to free-carrier generation, induced free-carrier absorption (at long wavelengths), self-phase modulation, and self-focusing.

In this Letter, we report the measurements of degenerate multiphoton absorption (MPA) coefficients and nonlinear refractive index in GaAs, in a broad mid-IR range, using the Z-scan technique.⁷ We utilized ~ 100 fs pulses from an optical parametric amplifier (Coherent Inc., OperA) pumped by a 0.8 μm Ti:sapphire regenerative amplifier (Coherent Inc., Legend). Combined with a difference frequency generator (at $\lambda > 3 \mu\text{m}$), we had tunability from 1.2 to 4.5 μm . The laser pulse repetition rate was 1 kHz, and the energy per pulse was up to $\sim 200 \mu\text{J}$. To minimize experimental error, we performed careful characterization of the laser pulse duration at each wavelength. Also, we used a spatial filter to produce a smooth Gaussian beam distribution. The samples were 350 μm thick semi-insulating GaAs

(110) wafers from AXT. The transmitted optical pulses were detected by a large-area pyroelectric detector placed in the far field of the focal beam spot with either a small aperture or no aperture. Transmission was measured as a function of sample position z along the beam. The incident beam intensity was monitored by a reference detector. The MPA coefficients and n_2 were obtained by analyzing open- and closed-aperture measurements, respectively.⁷

Raw results of Z-scan measurements at 1.68 and 2.30 μm are shown in Figs. 1(a) and 1(b). The laser beam was focused by using a CaF_2 lens with a focal length of 20 cm. At 1.68 (2.30) μm , the average focused spot size, measured by a knife-edge technique, was $w = 78.9$ (96.7) μm ($1/e^2$ intensity radius), energy per pulse 0.0315 (0.210) μJ , and pulse duration 111 (128) fs, corresponding to a peak on-axis incoming intensity of $I_{in} = 2.90$ (11.2) GW/cm^2 . The electric-field polarization was aligned along the [110] crystallographic direction of GaAs. At 1.68 μm , 2PA is the dominant nonlinear absorption process, which leads to the strong transmission dip at the focus ($z=0$) for the open-aperture data. The apparent asymmetry of the peak and the valley in the closed-aperture data shows contributions from both nonlinear refraction and 2PA. In contrast, at 2.30 μm , the peak and the valley are more symmetric in the closed-aperture data, which indicates that the n_2 effect is dominant. While n_2 remains about the same (see below), 2PA is negligible at this wavelength and 3PA ($\chi^{(5)}$ -related effect) is relatively weak at the input intensity.

MPA coefficients were calculated from Z-scans in the following way. We assume that only one type of MPA dominates for a given wavelength. Then, the optical intensity, $I(z, r, t)$ can be described by

$$\frac{dI(z, r, t)}{dz} = -\alpha_N I(z, r, t)^N, \quad (1)$$

where z is propagation distance, r transverse coordinate, t time, and α_N an N -photon absorption coefficient.

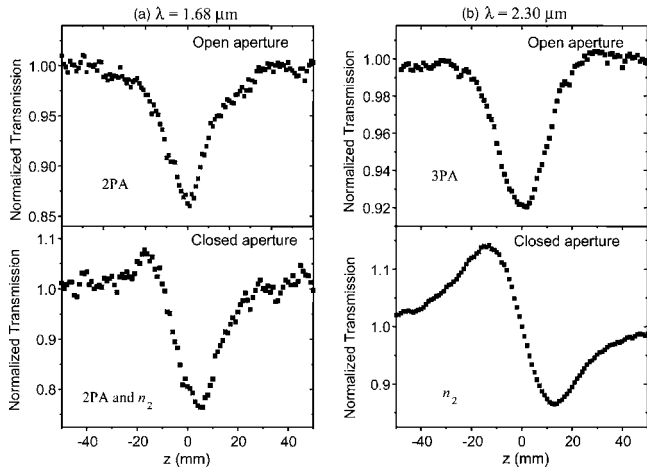


Fig. 1. Normalized transmission data obtained in open and closed-aperture Z scans (a) at $\lambda=1.68 \mu\text{m}$ and (b) at $2.30 \mu\text{m}$.

cient. For example, α_2 stands for 2PA coefficient β , and α_3 for 3PA coefficient γ . By integrating this equation over z , r , and t , we can find the transmitted pulse energy as a function of the peak incoming intensity I_{in} , and thus normalized transmission T/T_0 , where T_0 is the transmission in the low intensity limit. In general, the analytical solution for Eq. (1) is rather complicated. However, when $(T-T_0)/T_0 \ll 1$, it is straightforward to show by simple integration of Eq. (1) that, in the case of Gaussian laser pulses (in space and time),

$$\frac{T_0}{T} = 1 + \frac{1}{N^{3/2}} \alpha_N I_{in}^{N-1} l, \quad (2)$$

where l is the sample thickness. Hence, near the origin, (T_0/T) versus I_{in} is a linear function (2PA), parabola (3PA), cubic parabola (4PA), etc. This allowed us to distinguish MPA processes of different orders when we changed the laser wavelength. In general, MPA coefficients were deduced by best fitting the numerical solution of Eq. (1) to the experimental data for every open-aperture Z-scan in the whole range of transmission change, not only $(T-T_0)/T_0 \ll 1$.

At $1.68 \mu\text{m}$ the quantity $1/T$ is linearly dependent on the input intensity (Fig. 2), which indicates that it is the 2PA process that dominates; the result of the best fit is $\beta=2.5 \pm 0.2 \text{ cm/GW}$ at $1.68 \mu\text{m}$, which is consistent with $\beta \approx 3 \text{ cm/GW}$ obtained at $1.7 \mu\text{m}$ in Ref. 1. At $2.3 \mu\text{m}$, the curve near the origin is a quadratic function, i.e., the 3PA process is dominant. We obtained $\gamma=0.35 \pm 0.5 \text{ cm}^3/\text{GW}^2$ by numerically fitting the data. At $\lambda=3.47 \mu\text{m}$ (beyond the 3PA cutoff wavelength), transmission did not vary measurably for $I_{in} < 10 \text{ GW/cm}^2$, since neither 2PA nor 3PA are present. At much higher intensities, however, the nonlinear absorption becomes evident (inset, Fig. 2), which we attribute to 4PA and 5PA processes combined; $3.47 \mu\text{m}$ is on the boundary between these two effects. A numerical fit to the data indicates that no single nonlinear absorption process is dominant at this wavelength.

Figure 3 plots our experimental results for 2PA and 3PA coefficients in the $1.3\text{--}2.6 \mu\text{m}$ wavelength range. The 2PA coefficient at $1.06 \mu\text{m}$ (26 cm/GW) from Ref. 8 is shown for comparison. The solid curves represent theoretical results based on scaling laws derived from the two-band theory of MPA in direct bandgap semiconductors.⁹ When going from longer to shorter wavelengths, we observed a very steep increase of the total MPA near $1.75 \mu\text{m}$, due to the 3PA-to-2PA transition (the photon energy at $1.75 \mu\text{m}$ is close to half of the GaAs bandgap energy $E_g=1.42 \text{ eV}$).

Using a $2.0 \mu\text{m}$ pump, we measured the anisotropy of the degenerate 3PA coefficient in GaAs. Figure 4 shows the 3PA coefficient, γ , as a function of the angle θ between the electric-field polarization and the [001] direction. We obtained the curve by rotating the sample azimuthally in 10° increments about the [110] axis and taking Z-scans. Our experimental data were fitted with the following expression:

$$\gamma(\theta) = a + b \cos 2\theta + c \cos 4\theta, \quad (3)$$

where $a=0.224 \pm 0.001$, $b=-0.021 \pm 0.001$, and $c=-0.020 \pm 0.001$. This is the lowest-order Fourier series expansion that gives satisfactory fitting and matches the GaAs symmetry ($43m$). One can see from Fig. 4 that γ is maximized at polarization directions, close to $[1\bar{1}1]$ and $[1\bar{1}\bar{1}]$ of GaAs ($\theta=55^\circ$ and 125°). The relative min-max variation of γ in our case is $\sim 30\%$. Similar angular dependence was obtained in Ref. 10 for the 2PA coefficient, β , in (110) GaAs at $1.06 \mu\text{m}$ pump: β had a minimal value with polarization along [001], was maximized at [111], and had an intermediate value at [110] ($\theta=90^\circ$), with relative min-max variations of $\sim 40\%$.

We obtained n_2 data by analyzing closed-aperture Z-scan measurements at different wavelengths.⁷ The measured n_2 dispersion (polarization along [110] in

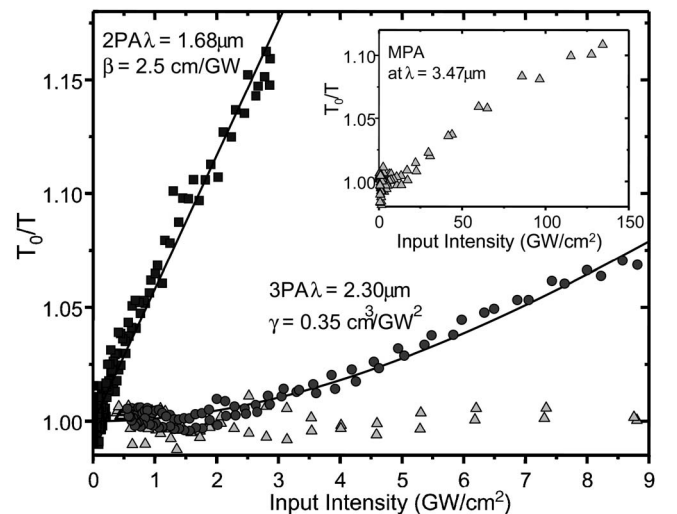


Fig. 2. Experimental data and best-fit curves (solid curves) for the normalized inverse nonlinear transmission (T_0/T) versus incoming peak intensity at $\lambda=1.68 \mu\text{m}$ (filled squares), $2.30 \mu\text{m}$ (filled circles), and $3.47 \mu\text{m}$ (open triangles). The inset shows the nonlinear transmission curve for $3.47 \mu\text{m}$ at much higher intensities.

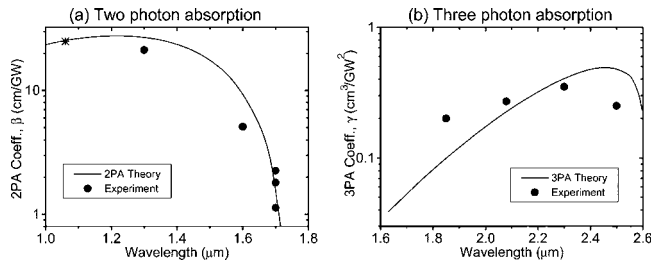


Fig. 3. Experimental data and theoretical curves (solid curves) of (a) 2PA and (b) 3PA coefficients versus wavelength (polarization along [110] of GaAs). The 2PA coefficient for $1.06 \mu\text{m}$ (*) was taken from the literature.⁸

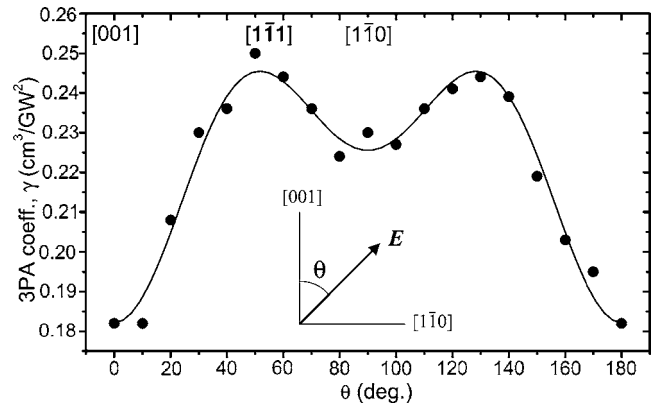


Fig. 4. Experimental data (filled circles) and numerical fit (solid curve) of the 3PA coefficient at $2 \mu\text{m}$ as a function of the angle θ between the optical polarization and the [001] axis.

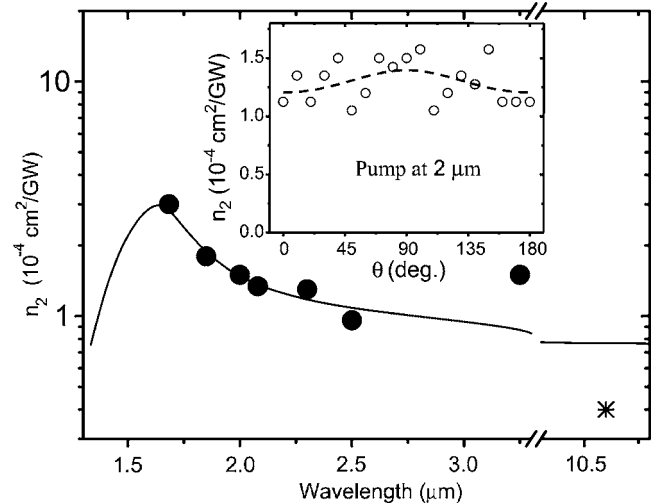


Fig. 5. Experimental data (filled circles) and theoretical curve (solid curve) of nonlinear refractive index n_2 versus wavelength (polarization along [110] in GaAs). n_2 for $10.6 \mu\text{m}$ (*) was obtained from the literature.¹¹ The inset shows results of n_2 anisotropy measurements and a numerical fit (dashed curve) to experimental data.

GaAs) is shown in Fig. 5. n_2 at $10.6 \mu\text{m}$ ($0.4 \times 10^{-4} \text{ cm}^2/\text{GW}$) obtained from Ref. 11 is included for comparison. A theoretical curve based on a two-band model of a semiconductor is also presented. It is

based on formula (44) of Ref. 12, with the value for the constant, $K' = 0.94 \times 10^{-8}$, derived from first principles. Our experimental results confirm theoretical predictions that there is little dispersion of n_2 at low ($< E_g/2$) photon energies. We measured the angular dependence of n_2 at $\lambda = 2 \mu\text{m}$ by doing Z scans at different θ and fitted the data with the functional form of Eq. (3) (inset, Fig. 5). We found that the relative max-min variation of the n_2 coefficient was $\sim 16\%$. However, clear angular dependence was obscured by experimental uncertainty of $\Delta n_2/n_2 = \pm 15\%$. The observed variation of n_2 was less than the theoretical prediction $n_2([110])/n_2([001]) \approx 2$ near $\lambda = 2 \mu\text{m}$ in Ref. 13.

In conclusion, we used femtosecond laser pulses in a broad range of infrared wavelengths to measure 2PA and 3PA coefficients and the nonlinear refractive index in GaAs. We found that there is agreement to within less than a factor of two between our measured nonlinear optical coefficients (β , γ and n_2) and theoretical predictions based on first principles. We found clear evidence of 3PA anisotropy, with γ being maximized at [111] direction of GaAs.

This work was supported by DARPA under grant FA9550-04-1-0465 and by NSF CAREER award 0449426. Y.-S. Lee's e-mail address is leeys@physics.oregonstate.edu.

References

1. A. Villeneuve, C. C. Yang, G. I. Stegeman, C. N. Ironside, G. Scelsi, and R. M. Osgood, *IEEE J. Quantum Electron.* **30**, 1172 (1994).
2. L. A. Eyres, P. J. Tourreau, T. J. Pinguet, C. B. Ebert, J. S. Harris, M. M. Fejer, L. Becouarn, B. Gerard, and E. Lallier, *Appl. Phys. Lett.* **79**, 904 (2001).
3. K. L. Vodopyanov, O. Levi, P. S. Kuo, T. J. Pinguet, J. S. Harris, M. M. Fejer, B. Gerard, L. Becouarn, and E. Lallier, *Opt. Lett.* **29**, 1912 (2004).
4. P. S. Kuo, K. L. Vodopyanov, M. M. Fejer, D. M. Simanovskii, X. Yu, J. S. Harris, D. Bliss, and D. Weyburne, *Opt. Lett.* **31**, 71 (2006).
5. G. Imeshev, M. E. Fermann, K. L. Vodopyanov, M. M. Fejer, X. Yu, J. S. Harris, D. Bliss, and C. Lynch, *Opt. Express* **14**, 4439 (2006).
6. K. L. Vodopyanov, M. M. Fejer, X. Yu, J. S. Harris, Y.-S. Lee, W. C. Hurlbut, and V. G. Kozlov, *Appl. Phys. Lett.* **89**, 141119 (2006).
7. M. Sheik-Bahae, A. A. Said, T.-H. Wei, D. J. Hagan, and E. W. van Stryland, *IEEE J. Quantum Electron.* **26**, 760 (1990).
8. A. A. Said, M. Sheik-Bahae, D. J. Hagan, T. H. Wei, J. Wang, J. Young, and E. W. van Stryland, *J. Opt. Soc. Am. B* **9**, 405 (1992).
9. B. S. Wherrett, *J. Opt. Soc. Am. B* **1**, 67 (1984).
10. R. DeSalvo, M. Sheik-Bahae, A. A. Said, D. J. Hagan, and E. W. Van Stryland, *Opt. Lett.* **18**, 194 (1993).
11. J. J. Wynne, *Phys. Rev.* **178**, 1295 (1969).
12. M. Sheik-Bahae, D. C. Hutchings, D. J. Hagan, and E. W. van Stryland, *IEEE J. Quantum Electron.* **27**, 1296 (1991).
13. D. C. Hutchings and B. S. Wherrett, *Phys. Rev. B* **52**, 8150 (1995).